Resonance tunneling through photonic quantum wells

Y. Jiang, C. Niu, and D. L. Lin
Department of Physics, State University of New York at Buffalo, Buffalo, New York 14260-1500
(Received 19 August 1998)

The band gap in photonic materials with periodic spatial modulation of refractive index greater than unity can actually be regarded as a potential barrier for photons. Similar to semiconductor quantum well systems due to the electronic band-gap mismatch, a photonic quantum well can be constructed by sandwiching a uniform medium between two photonic barriers. The transmission and reflection coefficients of light through the photonic quantum well are calculated by a modal expansion method with an *R*-matrix propagation algorithm. Resonance tunneling through the photonic quantum well structure is observed by varying either the well width or the frequency of incident light. Resonance peaks are found within the band-gap region, and indicate the existence of photon virtual states in the well. [S0163-1829(99)07815-7]

I. INTRODUCTION

Ever since the idea of photonic band structure was introduced[1,2] by analogy of photons in a periodic spatial dielectric structure to electrons in crystals, this area of research has received much attention because of the fundamental interest in localization of light and potential applications of the photonic band gap. It is well known that the electronic quantum well system is formed by electronic band mismatch and is of great interest in physical properties as well as in practical applications. It is possible to draw a complete analogy between electronic and photonic crystals because they both exhibit band gaps. Examples include the inhibition of spontaneous emission in solid-state physics and electronics,[1] as well as possible observation and application of strong Anderson localization of photons.[2] More recently, it is demonstrated that light extraction efficiency is significantly enhanced in spontaneous emission from a thin slab of two-dimensional (2D) photonic crystal.[3]

There has been a considerable amount of theoretical and experimental efforts in searching for the photonic material possessing band gap with notable results.[4–6] For three-dimensional (3D) photonic crystals, the first experimental observation of band gap was made in periodic face-centered cubic (fcc) dielectric structures.[4] But theoretical calculations by means of the vector plane-wave expansion indicate that no true gap extends throughout the whole Brillouin zone for the fcc structure,[5,6] as is explained by the symmetry consideration at *W* point in the Brillouin zone.

Several ways of breaking the symmetry at *W* point have been proposed. One of them is to introduce ''nonspherical atoms'' to the fcc structure. Numerical studies of this ''new photonic crystal'' show the existence of a full photonic band gap and the result is verified by experimental observations.[7] Another symmetry breaking at *W* point is to produce a diamond structure by introducing an fcc lattice to a second fcc structure, which also exhibits a full photonic band gap.[8] It is also found that the band-gap width is related to the degree of symmetry of the photonic structure. For 2D square and honeycomb lattices of circular cross-sectional rods, the band gap enlarges when the symmetry is reduced by adding a rod of smaller diameter into the center of each lattice unit cell.[9] The theoretical calculation of the band gap for 2D photonic crystals using the plane-wave expansion method finds very good agreement with experimental results, which are obtained by the technique of coherent microwave transient spectroscopy.[10]

In this paper, we investigate the resonance tunneling of light through a photonic quantum well system. We consider two photonic barriers with a uniform medium in between as a quantum well system for photons. A remark may be in order at this point. The tunneling problem becomes trivial if our system of photonic barriers is replaced by a superlattice-like structure composed of alternating layers of two dielectric materials. However, the 1D tunneling system is of little interest in practice because it is much more difficult to observe band gap effects in 1 D planar cavities than in 2D photonic crystals.[11] After all, it is the experiments carried out on 2D photonic crystals that have prompted interests in theoretical studies.[9,12–15]

There exist many mathematical techniques such as the plane-wave expansion,[5,6,8,16,17] the Korringa-Kohn- Rostoker method,[14,18,19] the augmented plane-wave method,[20] the on-shell theory of electron diffraction,[21] the *kp* method,[22] and so forth. Most of them are well known in the treatment of electronic band structures. In addition, a numerical technique based on the finite difference time-domain method has been introduced to calculate the photonic band structure of materials possessing Kerr nonlinearity.[23]

We choose, however, the modal expansion method with *R*-matrix propagation algorithm because it is inherently suitable for photonic crystals of finite thickness and is less demanding on computation resources.[12,13] It has been demonstrated that the calculated light transmission coefficient conforms well to the experimental data.[10] Furthermore, the vector nature of both electric and magnetic fields are fully taken into account in the modal expansion technique.[13] As a matter of fact, this is crucial in the calculation of photonic band structure because the scalar plane-wave expansion predicts a full band gap for pure fcc structures while only pseudoband gap actually exists.

II. THEORY

We consider a photonic quantum well system consisting of two thin slabs of 2D photonic crystal with uniform optical

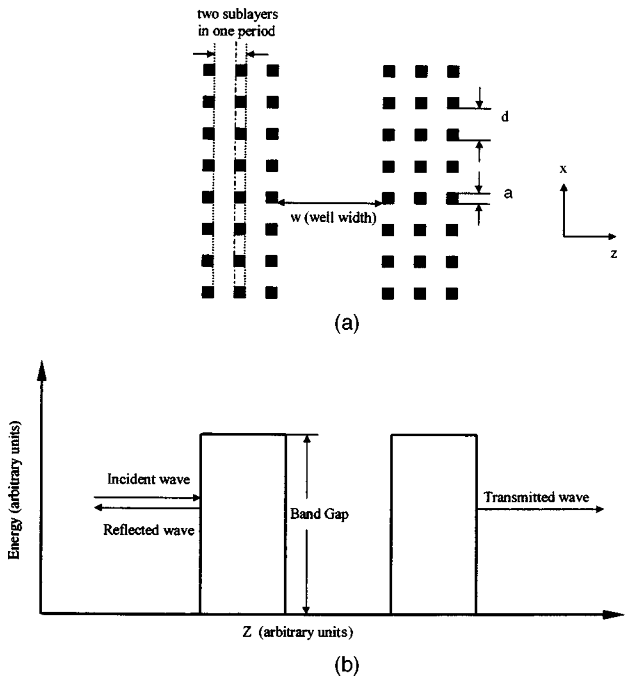

FIG. 1. The photonic quantum well structure. (a) Schematic diagram of the cross-sectional view for the physical arrangement. The rods are infinitely long in the y direction and infinitely periodic in the x direction. (b) The quantum well system as seen by incident photons with frequencies within the band gap.

medium in between. The slab of photonic crystal is an array of infinitely long dielectric cylinders with constant permittivity ε. For simplicity, the cross section of the cylinder is assumed to be a square of side length a. The spatial period of the array of cylinders is d. Figure 1(a) shows the geometry. The crystal is infinitely periodic in the $\hat{x}$ direction and the cylinders are placed along the $\hat{y}$ direction. The thickness is finite in the $\hat{z}$ direction. As a photon of frequency ω within the forbidden gap of the 2D photonic crystal falls on the surface, the slab of photonic crystal acts as a potential barrier. Physically, the quantum well system is shown in Fig. 1(b), in which the height of the barrier is taken to be the width of the band gap.

The photonic crystal can be described by a spatially variable permittivity $\varepsilon(\mathbf{r})$. In the 2D case, $\varepsilon(\mathbf{r})=\varepsilon(x,z)$. Following Ref. 13, we further divide the photonic crystal into sublayers in $\hat{z}$ direction such that within each sublayer, the permittivity is independent of z, i.e., $\varepsilon(\mathbf{r})=\varepsilon(x)$. The Maxwell's equation can then be solved within each sublayer, by the modal expansion in real space. Let us start with the Maxwell's equations

$$\nabla\times\mathbf{E}(\mathbf{r})=i\frac{\omega}{c}\mathbf{H}(\mathbf{r}), \tag{1a}$$

$$\nabla\times\mathbf{H}(\mathbf{r})=-i\frac{\omega}{c}\varepsilon(\mathbf{r})\mathbf{E}(\mathbf{r}), \tag{1b}$$

where ω is the angular frequency. Because of symmetry, $\mathbf{E}(\mathbf{r})$ and $\mathbf{H}(\mathbf{r})$ do not depend on y and consequently we have $\mathbf{E}(\mathbf{r})=\mathbf{E}(x,z)$, $\mathbf{H}(\mathbf{r})=\mathbf{H}(x,z)$. The mathematical details of the formalism can be found in Ref. 13. In what follows, only essential steps are outlined.

Let us now divide one period of the crystal along x direction into N segments, i.e., $\Delta x=d/N$. After the elimination of z components H_z and E_z in Eq. (1), we obtain the coupled equations for E_x, E_y, H_x, and H_y as follows:

$$\frac{\partial E_x(x,z)}{\partial z}=\alpha H_y(x,z)+\beta\left\{\frac{H_y(x+\Delta x,z)-H_y(x,z)}{\varepsilon(x+\Delta x/2)}+\frac{H_y(x-\Delta x,z)-H_y(x,z)}{\varepsilon(x-\Delta x/2)}\right\}, \tag{2a}$$

$$\frac{\partial E_y(x,z)}{\partial z}=-\alpha H_x(x,z), \tag{2b}$$

$$\frac{\partial H_x(x,z)}{\partial z}=-\alpha\varepsilon(x)E_y(x,z)+\beta\{2E_y(x,z)-E_y(x+\Delta x,z)-E_y(x-\Delta x,z)\}, \tag{2c}$$

$$\frac{\partial H_y(x,z)}{\partial z}=\alpha\varepsilon(x)E_x(x,z), \tag{2d}$$

where we have defined $\alpha=i\omega/c$, $\beta=ic/\omega(\Delta x)^2$, and X to denote collectively all N discrete x coordinates. We now introduce the notation

$$\tilde{E}(x,z)=\begin{bmatrix}E_x(x,z)\\E_y(x,z)\end{bmatrix}, \tag{3a}$$

$$\tilde{H}(x,z)=\begin{bmatrix}H_x(x,z)\\H_y(x,z)\end{bmatrix}, \tag{3b}$$

$$A(x,z)=\begin{bmatrix}\tilde{E}(x,z)\\\tilde{H}(x,z)\end{bmatrix}, \tag{3c}$$

in which E_x, E_y, H_x, and H_y are N-dimensional vectors and A is a $4N$-dimensional vector. In terms of matrices, Eq. (2) can be written as

$$\frac{\partial A}{\partial z}=M(x)A(x,z), \tag{4}$$

where the matrix M is independent of z within each sublayer. After the diagonalization of matrix M, we find the solution of Eq. (4) as

$$A(X,z)=\begin{bmatrix}\tilde{E}(X,z)\\\tilde{H}(X,z)\end{bmatrix}=S(X)e^{\Lambda z}C=\begin{bmatrix}S_{11}&S_{12}\\S_{21}&S_{22}\end{bmatrix}\begin{bmatrix}e^{\lambda_1 z}&0\\0&e^{\lambda_2 z}\end{bmatrix}\begin{bmatrix}c_1\\c_2\end{bmatrix}, \tag{5}$$

where Λ are eigenvalues of $M(X)$, and $S(X)$ is a square matrix whose columns are eigenvectors of $M(X)$.

The R matrix is defined by

$$\begin{bmatrix} \tilde{E}(X,z_1) \\ \tilde{E}(X,z_2) \end{bmatrix} = R(z_2-z_1) \begin{bmatrix} \tilde{H}(X,z_1) \\ \tilde{H}(X,z_2) \end{bmatrix}, \tag{6}$$

which relates the electric field to the corresponding magnetic field at the sublayer boundaries. From Eqs. (5) and (6), we can express $R(z_2-z_1)$ in terms of S and Λ as

$$\begin{aligned} R(z_2-z_1) &= \begin{bmatrix} R_{11}(z_2-z_1) & R_{12}(z_2-z_1) \\ R_{21}(z_2-z_1) & R_{22}(z_2-z_1) \end{bmatrix} \\ &= \begin{bmatrix} S_{11} & S_{12} \\ S_{11}e^{\lambda_1(z_2-z_1)} & S_{12}e^{\lambda_2(z_2-z_1)} \end{bmatrix} \\ &\quad \times \begin{bmatrix} S_{21} & S_{22} \\ S_{21}e^{\lambda_1(z_2-z_1)} & S_{21}e^{\lambda_2(z_2-z_1)} \end{bmatrix}^{-1}. \end{aligned} \tag{7}$$

The recursion formula for the R-matrix algorithm can be derived from Eq. (7). If both $R(z_2-z_1)$ and $R(z_3-z_2)$ are known, it is straightforward to derive $R(z_3-z_1)$ from Eq. (6) with the continuity of electric and magnetic fields at z_2. The results are

$$\begin{aligned} R_{11}(z_3-z_1) = R_{11}(z_3-z_2) + R_{12}(z_3-z_2)[R_{11}(z_2-z_1) \\ - R_{22}(z_3-z_2)]^{-1}R_{21}(z_3-z_2), \end{aligned} \tag{8a}$$

$$\begin{aligned} R_{12}(z_3-z_1) = -R_{12}(z_3-z_2)[R_{11}(z_2-z_1) \\ - R_{22}(z_3-z_2)]^{-1}R_{12}(z_2-z_1), \end{aligned} \tag{8b}$$

$$\begin{aligned} R_{21}(z_3-z_1) = R_{21}(z_2-z_1)[R_{11}(z_2-z_1) \\ - R_{22}(z_3-z_2)]^{-1}R_{21}(z_3-z_2), \end{aligned} \tag{8c}$$

$$\begin{aligned} R_{22}(z_3-z_1) = R_{22}(z_2-z_1) - R_{21}(z_2-z_1)[R_{11}(z_2-z_1) \\ - R_{22}(z_3-z_2)]^{-1}R_{12}(z_2-z_1). \end{aligned} \tag{8d}$$

III. RESONANCE TUNNELING

Each spatial period along the z direction is divided into two sublayers. The R matrix for each sublayer can be found from Eq. (7) separately. For one period of photonic crystal in the z direction, the R matrix can be found from the recursion algorithm (8). Repeating the above procedure, we can evaluate the R matrix R^b for the whole slab of the photonic barrier. The uniform medium or the well is treated as a special case of photonic crystal with $\varepsilon(\mathbf{r}) = \text{constant}$, the R matrix R^w for the well then follows from Eq. (2) directly. The complete R matrix $\Re = R^{bwb}$ for the whole quantum well system is found by adding the second barrier. Thus,

$$R_{11}^{bwb} = R_{11}^b + R_{12}^b[R_{11}^w + R_{12}^w(R_{11}^b - R_{22}^w)^{-1}R_{21}^w - R_{22}^b]^{-1}R_{21}^b, \tag{9a}$$

$$\begin{aligned} R_{12}^{bwb} = R_{12}^b[R_{11}^w + R_{12}^w(R_{11}^b - R_{22}^w)^{-1}R_{21}^w - R_{22}^b]^{-1} \\ \times R_{21}^b R_{12}^w (R_{11}^b - R_{22}^w)^{-1}R_{12}^b, \end{aligned} \tag{9b}$$

$$\begin{aligned} R_{21}^{bwb} = R_{21}^b(R_{11}^b - R_{22}^w)^{-1}R_{21}^w[R_{11}^w + R_{12}^w(R_{11}^b - R_{22}^w)^{-1} \\ \times R_{21}^w - R_{22}^b]^{-1}R_{21}^b, \end{aligned} \tag{9c}$$

$$\begin{aligned} R_{22}^{bwb} = R_{22}^b - R_{21}^b(R_{11}^b - R_{22}^w)^{-1}R_{12}^b \\ + R_{21}^b(R_{11}^b - R_{22}^w)^{-1}R_{21}^w[R_{11}^w + R_{12}^w(R_{11}^b - R_{22}^w)^{-1} \\ \times R_{21}^w - R_{22}^b]^{-1}R_{12}^w(R_{11}^b - R_{22}^w)^{-1}R_{12}^b. \end{aligned} \tag{9d}$$

On the left-hand side of the photonic well system, the electromagnetic field is a superstition of incident wave and reflected wave. On the right, the electromagnetic field is the transmitted wave. Applying Eq. (9) to the whole quantum well system we find

$$\begin{bmatrix} \tilde{E}^t(X) \\ \tilde{E}^r(X) + \tilde{E}^{inc}(X) \end{bmatrix} = \Re \begin{bmatrix} \tilde{H}^t(X) \\ \tilde{H}^r(X) + \tilde{H}^{inc}(X) \end{bmatrix}, \tag{10}$$

where $\tilde{E}^{inc}(X)$, $\tilde{H}^{inc}(X)$; $\tilde{E}^r(X)$, $\tilde{H}^r(X)$; and $\tilde{E}^t(X)$, $\tilde{H}^t(X)$ are incident, reflected and transmitted electric, and magnetic fields, respectively. To find the relation between $\tilde{E}(X)$ and $\tilde{H}(X)$ in the homogeneous region, we note that in the momentum space

$$E(\mathbf{r}) = \frac{1}{(2\pi)^2}\int d^2K E(\mathbf{K}) e^{i\mathbf{K}\mathbf{r}_1} e^{isz}, \tag{11a}$$

$$H(\mathbf{r}) = \frac{1}{(2\pi)^2}\int d^2K H(\mathbf{K}) e^{i\mathbf{K}\mathbf{r}_1} e^{isz}, \tag{11b}$$

where $r_1 = (x,y)$, $s = [\varepsilon(\omega/c)^2 - K^2]^{1/2}$ and K is the 2D wave vector, the relation is particularly simple and is given by

$$\tilde{H}(K) = T(K,s)\tilde{E}(K), \tag{12a}$$

$$T(K,s) = \begin{bmatrix} -K_xK_y \Big/ \frac{\omega}{c}s & -(s^2+K_y^2) \Big/ \frac{\omega}{c}s \\ (s^2+K_x^2) \Big/ \frac{\omega}{c}s & K_xK_y \Big/ \frac{\omega}{c}s \end{bmatrix}. \tag{12b}$$

If the incident wave propagates along the z axis, the transmitted and reflected waves will, by symmetry, also propagate in the z direction and the matrix $T(K,s)$ becomes very simple. Hence, we can express the incident, transmitted and reflected magnetic fields $\tilde{H}^{inc}(K), \tilde{H}^t(K), \tilde{H}^r(K)$ in terms of the corresponding electric fields as

$$\tilde{H}^{inc}(K) = T_+\tilde{E}^{inc}(K), \tag{13a}$$

$$\tilde{H}^t(K) = T_+\tilde{E}^t(K), \tag{13b}$$

$$\tilde{H}^r(K) = T_-\tilde{E}^r(K), \tag{13c}$$

where we have defined

$$T_+ = \begin{bmatrix} 0 & -\mathbf{I} \\ \mathbf{I} & 0 \end{bmatrix}, \tag{14a}$$

$$T_- = \begin{bmatrix} 0 & \mathbf{I} \\ -\mathbf{I} & 0 \end{bmatrix}, \tag{14b}$$

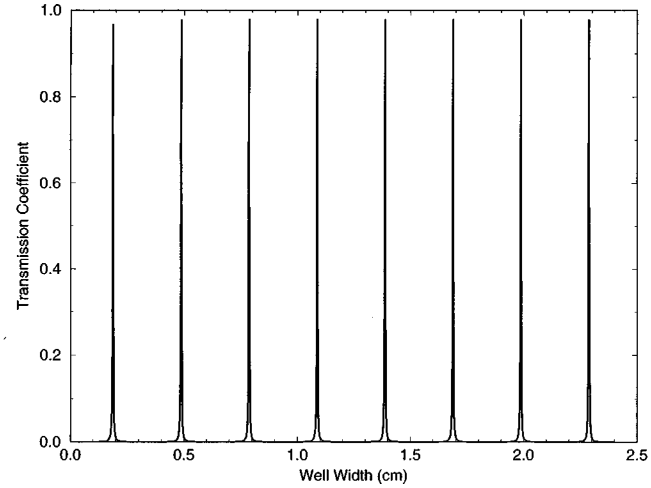

FIG. 2. Transmission coefficient versus the well width for a fixed frequency of 50 GHz. The incident wave is polarized parallel to cylinder axes.

with the $N\times N$ unit matrix $\mathbf{I}$. The corresponding relations in real space are obtained from Eq. (13) directly by the discrete Fourier transformation

$$\tilde{E}(X)=F(X,K)\tilde{E}(K), \tag{15a}$$

$$\tilde{H}(X)=F(X,K)\tilde{H}(K), \tag{15b}$$

where $F(X,K)$ is a Fourier-transformation matrix. Thus, we have

$$\tilde{H}^{inc}(X)=\overline{T_+}\tilde{E}^{inc}(X), \tag{16a}$$

$$\tilde{H}^{t}(X)=\overline{T_+}\tilde{E}^{t}(X), \tag{16b}$$

$$\tilde{H}^{r}(X)=\overline{T_-}\tilde{E}^{r}(X), \tag{16c}$$

where we have defined the transformation

$$\overline{T_+}=F(X,K)T_+F^{-1}(X,K), \tag{17a}$$

$$\overline{T_-}=F(X,K)T_-F^{-1}(X,K). \tag{17b}$$

Substitute Eq. (16) into Eq. (10), we obtain

$$\begin{bmatrix} \Re_{11}\overline{T_+}-\mathbf{I} & \Re_{12}\overline{Z_-} \\ \Re_{21}\overline{Z_+} & \Re_{22}\overline{T_-}-\mathbf{I} \end{bmatrix} \begin{bmatrix} \tilde{E}^{t}(X) \\ \tilde{E}^{r}(X) \end{bmatrix} = \begin{bmatrix} -\Re_{12}\overline{Z_+}\tilde{E}^{inc}(X) \\ [\mathbf{I}-\Re_{22}\overline{Z_+}]\tilde{E}^{inc}(X) \end{bmatrix}. \tag{18}$$

Equation (18) may be solved for $\tilde{E}^{t}(X)$ and $\tilde{E}^{r}(X)$, from which we find the coefficients of transmission and reflection for electromagnetic waves incident on the photonic quantum well system.

IV. RESULTS AND DISCUSSION

In the numerical calculation, we choose parameters for the 2D photonic crystal similar to those in experimental measurement.[10] The cylinders of the photonic crystal are made of aluminum ceramics with a dielectric constant 8.9. The lattice constant is taken to be 1.87 mm, and the side of the cylinder's square cross section is 0.74 mm. For the uniform medium in the well we assume the vacuum for simplicity. If the electric field is polarized parallel to the rod axis, both theoretical calculation[12] and experimental measurement[10] show that the photonic band gap is between 45 and 70 GHz for a photonic barrier of seven layers of aluminum ceramic rods.

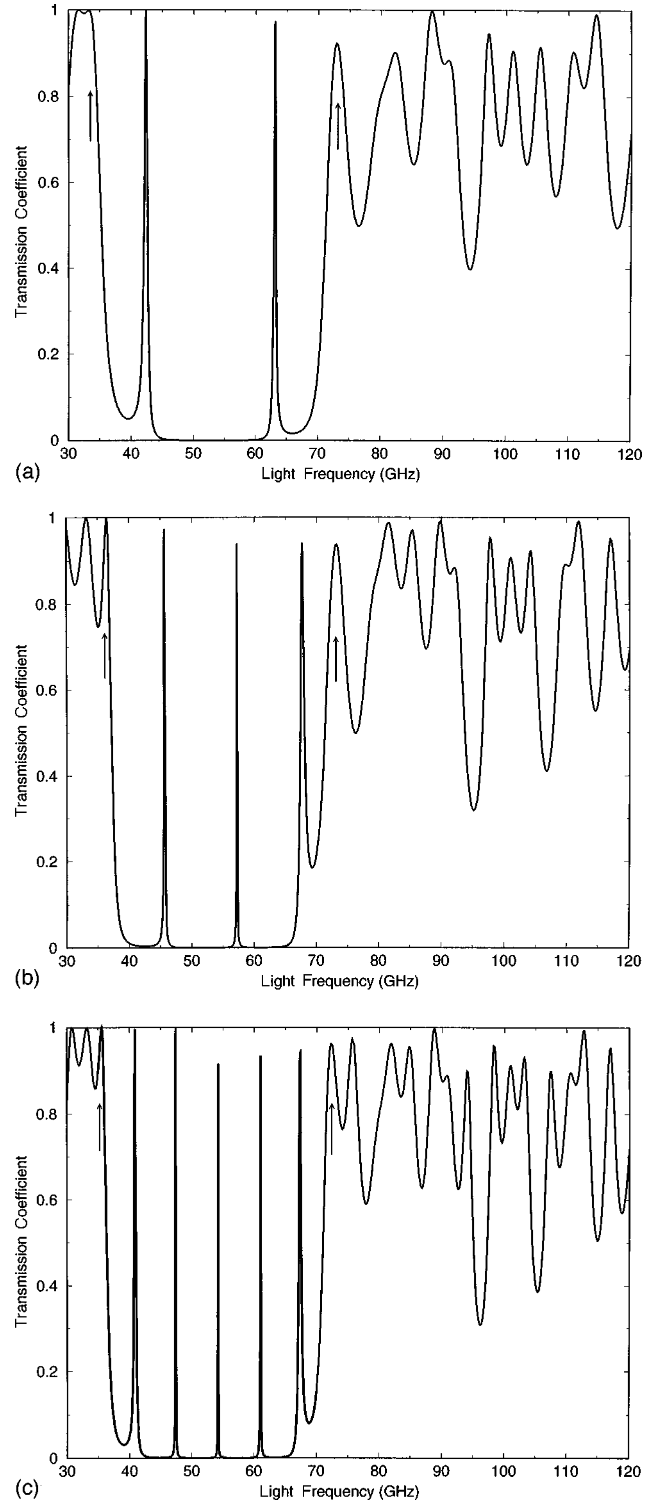

FIG. 3. Transmission coefficient versus the incident light frequency for a well width (a) $w=3$ mm, (b) $w=9$ mm and (c) $w=18$ mm. The polarization of the incident wave is parallel to the cylinder axes. Arrows indicate the position of band edges.

Our numerical work indicates that the transmission coefficient is vanishingly small for seven-layer barriers. Thus, we take three-layer barriers instead. As we shall see from numerical studies later, changes in thickness of the photonic crystal may modify somewhat the position and size of the photonic band gap. If the incident wave of frequencies between 40 and 70 GHz enters a slab of such 2D photonic crystals, the transmission rate still falls sharply with the penetration depth to nearly zero. Thus, the slab generally blocks incident light. The situation becomes very different, however, when light falls on a quantum well system as sketched in Fig. 1(b). More specifically, we consider a photonic quantum well system consisting of two slabs of 2D barriers separated by a homogenous region of width w. Each barrier contains three layers of aluminum ceramic rods stacked in the z direction. These rods are infinitely long in the y direction and arranged infinitely periodic in the x direction. Although incident light of frequencies between 40 and 70 GHz is blocked by the barrier, but transmission occurs at resonant frequencies of the quantum well system. In other words, resonance tunneling can be observed in such systems. To check our calculation, we have reproduced the results of Ref. 12 for a single barrier.

As it is known from both experiments and calculations, a much wider band gap opens up for the parallel polarization than for the perpendicular polarization of the E field.[10,12] Thus, we only consider the case of parallel polarization in our numerical study. For the incident wave with a fixed frequency of 50 GHz, we calculate the reflection coefficient r and transmission coefficient t across the photonic quantum well system as a function of the width w of photonic well. These coefficients are computed from Eq. (18) independently and numerical results are checked against the relation $r+t=1$ for every case. The error is consistently within 0.5%. Figure 2 depicts the variation of the transmission coefficient with the well width w. It is clearly observed that the resonance peaks occur regularly as w increases. The complete transmission is approximately determined by the condition $Kw=n\pi$, $n=1,2,3,\ldots$. This implies that there exist photon virtual states in the well.

We now investigate the variation of t with the incident light frequency for a given well width. The transmission and reflection coefficients are calculated as a function of the incident frequency from 30 to 120 GHz for a fixed well width. The polarization of the incident wave is chosen to be along the cylinder axis in all cases. Results for three different well widths $w=3$, 9, and 18 mm are presented in Fig. 3, in which the band edges are marked by arrows. As is observed from the three cases in Fig. 3, the band gap for the structure under consideration is consistent with experimental results of Ref. 10. The phenomenon of resonance tunneling through a photonic quantum well is thus similar to that in the electronic case. A number of resonance states exist in the photonic well. These virtual levels are characterized by frequencies $f_n=nc/w$, where n is integer, and hence are equally spaced. Whenever the frequency of the incident wave coincides with f_n, resonance occurs and the transmission reaches its peak value. As the well width increases, the spacing between resonant states narrows. Consequently, more resonance peaks appear. This is clearly shown in Fig. 3(a), 3(b), and 3(c).

The resonance peaks are very sharp with a line-width of about 70 MHz. For the past couple of decades, the electronic quantum well structure has witnessed wide applications in many areas. It is quite plausible to expect that the photonic quantum well system can also find applications in practical cases. Therefore, experimental investigation is urged to explore the resonance tunneling through photonic quantum well structures. As a matter of fact, there should not be essential difficulty to carry out experiments on the observation of resonance tunneling effects with the coherent microwave transient spectroscopic technique.[10]

It is also noted from Fig. 3 that at the band edges, the tunneling peaks appear wider than those in the gap. This is because the conduction bands help enhance the transmission rate, and hence result in a wider width of the peak.

We have applied the modal expansion method with an R-matrix algorithm to calculate the light transmission and reflection coefficients through a photonic quantum well light system. Resonant tunneling is found when the incident light frequency $f_n=nc/w$, just like the electronic tunneling through semiconductor quantum well systems. Experimental exploration of the phenomenon is suggested. The R-matrix algorithm proves to be a stable and efficient method for numerical studies of photonic crystals. It is particularly suitable for systems of finite size. In our opinion, the technique will be useful in most theoretical investigations on photonic crystal applications.

[1] E. Yablonovitch, Phys. Rev. Lett. **58**, 2059 (1987).

[2] S. John, Phys. Rev. Lett. **58**, 2486 (1987).

[3] S. Fan, P. R. Villeneuve, and J. D. Joannopoulos, Phys. Rev. Lett. **78**, 3294 (1997).

[4] E. Yablonovitch and T. J. Gmitter, Phys. Rev. Lett. **63**, 1950 (1989).

[5] K. M. Leung and Y. F. Liu, Phys. Rev. Lett. **65**, 2646 (1990).

[6] Z. Zhang and S. Satpathy, Phys. Rev. Lett. **65**, 2650 (1990).

[7] E. Yablonovitch, T. J. Gmitter, and K. M. Leung, Phys. Rev. Lett. **67**, 2295 (1991).

[8] K. M. Ho, C. T. Chan, and C. M. Soukoulis, Phys. Rev. Lett. **65**, 3152 (1990).

[9] C. M. Anderson and K. P. Giapis, Phys. Rev. Lett. **77**, 2949 (1996).

[10] W. M. Robertson, G. A. Arjavalingam, R. D. Meade, K. D. Brommer, A. M. Rappe, and J. D. Joannopoulos, Phys. Rev. Lett. **68**, 2023 (1992).

[11] T. Baba and M. Koma, Jpn. J. Appl. Phys., Part 1 **34**, 1405 (1995).

[12] J. M. Elson and P. Tran, J. Opt. Soc. Am. A **12**, 1765 (1995).

[13] J. M. Elson and P. Tran, Phys. Rev. B **54**, 1711 (1996).

[14] Sajeev John and R. Rangarajan, Phys. Rev. B **38**, 10 101 (1988).

[15] T. Baba and T. Matsuzaki, Jpn. J. Appl. Phys., Part 1 **34**, 4496 (1995).

[16] S. Satpathy, Z. Zhang, and M. R. Salehpour, Phys. Rev. Lett. **64**, 1239 (1990).
[17] K. M. Leung and Y. F. Liu, Phys. Rev. B **41**, 10 188 (1990).
[18] K. M. Leung and Y. Qiu, Phys. Rev. B **48**, 7767 (1993).
[19] X. Wang, X. G. Zhang, Q. Yu, and B. N. Harmon, Phys. Rev. B **47**, 4161 (1992).
[20] N. Economou and A. Zdetsis, Phys. Rev. B **40**, 1334 (1989).
[21] J. B. Pentry and A. MacKinnon, Phys. Rev. Lett. **69**, 2772 (1992).
[22] N. F. Johnson and P. M. Hui, Phys. Rev. B **48**, 10 118 (1993).
[23] P. Tran, Phys. Rev. B **52**, 10 673 (1995).